HiSST: 4th International Conference on
High-Speed Vehicle Science & Technology

22–26 September 2025, Tours, France

CEAS
Council of European Aerospace Societies

Detached eddy simulation of Callisto vehicle during subsonic retro-propulsion descent

Tobias Ecker[†]

Abstract

The estimation of aerothermal loads along the trajectory are a design driving factor during launcher development both for expendable as well as reusable space launch systems. The thermal loads directly influence TPS design and the fore the vehicle mass and mission performance. For reusable launch vehicles (RLV) (e.g. Falcon9, Spaceship) the thermal loads and the selected TPS materials might have direct impact on the refurbishment effort and concurrent launch cost. For the CALLISTO vehicle the highest heat fluxes are mainly during the subsonic retro-propulsion phase due to heating from hot exhaust gases and heated air in proximity of the aft bay and on the exposed structures like legs and fins. In the presented study we conducted computational fluid dynamics (CFD) study using the Detached Eddy Simulation (DES) approach in order to determine the unsteady and time-averaged aerothermal loads on the vehicle at beginning of the demo flight powered descent at M=0.8. The study was conducted for 0.3 s of flow time after the start up period. Subsequently the time-averaged loads were evaluated and compared to the baseline RANS model for the different vehicle interfaces. Based on the simulation results it can be observed that there are (1) clear differences between RANS and DES for plume core length, (2) strong loads fluctuations (aerodynamic and thermal) due to large scale turbulent structures in the plume but also (3) that the qualitative loads distribution is similar in average when compared to the RANS results. While large scale turbulent structures heavily influence the instantaneous thermal loads on the different vehicle interfaces the time-averaged results show a qualitative similar distribution to the RANS results for the same conditions. However the impact of the higher instantaneous loads may strongly depend on the material properties and the thermal mass of the underlying structure and the TPS system.

Keywords: *plume, aerothermal loads, subsonic retro-propulsion, launcher*

Nomenclature

Latin
M – Mach number
T – Temperature
Q – Heat flux
U – Velocity
Nu – Nusselt number
p – Pressure
C_p – Pressure coefficient

Greek
ρ – Density

Subscripts
w – Wall
∞ – freestream

1. Introduction

The estimation of aerothermal loads along the trajectory are a design driving factor during launcher development both for expendable as well as reusable space launch systems[1]. The thermal loads directly influence TPS design and the fore the vehicle mass and mission performance. For reusable launch vehicles (RLV) (e.g. Falcon9, Spaceship) the thermal loads and the selected TPS materials might have direct impact on the refurbishment effort and concurrent launch cost. In order to advance knowledge on RLV relevant technologies the German Aerospace Center (DLR), the Japan Aerospace Exploration Agency (JAXA) and the French Space Agency (CNES) entered into a collaboration agreement. This allows a significant increase of the organisational knowledge at a technical and economic level. This collaboration includes in

[†] *German Aerospace Center, Institute of Aerodynamics and Flow Technology, tobias.ecker@dlr.de*

particular a vertical take-off and vertical landing (VTVL) reusable sub-scale launcher first stage demonstrator. The vehicle is called CALLISTO, which stands for "Cooperative Action Leading to Launcher Innovation in Stage Toss back Operations". For the CALLISTO vehicle the highest heat fluxes are mainly during the subsonic retro-propulsion phase due to heating from hot exhaust gases and heated air in proximity of the aft bay and on the exposed structures like legs and fins. The development of the plume extension is different for the considered re-entry, when compared to Falcon 9, or other studies presented previously. As shown by Dumont et al.[2] the plume remains relatively concentrated at the aft end of the vehicle due to high atmospheric pressure and only very low fractions of actual exhaust gas species enclosing the vehicle. The subsonic phase is present for almost all currently proposed reusable launchers, even though the main focus so far has been on the supersonic or hypersonic[1, 3, 4] retro-propulsion phase. Asides from CALLISTO first launcher studies on subsonic retro-propulsion, numerically[5] and experimentally[6, 7] were conducted at DLR during the RETALT and RETPRO projects. Subsonic retro-propulsion experiments with combustion conducted at the DLR in Cologne by Marwege et al.[6] showed a strong unsteady behaviour. Marwege et al.[7] similarly reported a strongly dynamic behaviour and the occurrence of large scale structures in a similar study on cold air jets emerging from a launcher configuration.

Figure 1. Artistic impression of the CALLISTO vehicle. DES results visualizing the large scale structures using the Q criterion colored by temperature.

In the presented study we conducted computational fluid dynamics (CFD) study using the Detached Eddy Simulation (DES) approach in order to determine the unsteady and time-averaged aerothermal loads on the vehicle at beginning of the demo flight powered descent at M=0.8. The study was conducted for 0.3 s of flow time after the start up period. An artistic impression of the large and small scale flow structures in the plume and around the vehicle is shown in figure 1. Subsequently the time-averaged loads were evaluated and compared to the baseline RANS model for the different vehicle interfaces. Based on the simulation results it can be observed that there are (1) clear differences between RANS and DES for plume core length, (2) strong loads fluctuations (aerodynamic and thermal) due to large scale turbulent structures in the plume but also (3) that the qualitative loads distribution is similar in average when compared to the RANS results.

2. CALLISTO vehicle

2.1. Vehicle design

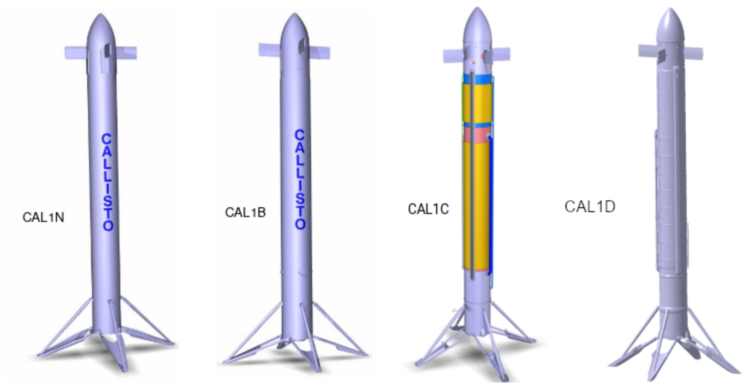

Figure 2. CALLISTO aeroshape evolution

During the project the CALLISTO aeroshape has changed in various ways. A comparison of previous outer mold lines with the shape CAL1B (phase B shape) can be found in [8]. From Phase B onwards the shape changes were mostly limited to detailed design of legs, cable ducts and piping as well as changes due to TPS application and product design, however larger changes were seen in phase D regarding the legs. A visualisation of the shape evolution is shown in figure 2. For this paper only the aeroshape CAL1C is considered as it is the main aeroshape used for the CALLISTO aerodynamic and aerothermal databases[9]. The aeroshape evolution and related aerodynamic properties are further detailed in [10]. A detailed comparison of CAL1C-CAL1D aeroshape transition and its negligible influence on the predicted aerothermal loads can be found in Ertl et al. [11].

The Reusable Sounding Rocket (RSR) engine used for CALLISTO is developed by JAXA in cooperation with Mitsubishi Heavy Industries (MHI) and is based on LOX/LH_2 fuel. The RSR engine uses an expander bleed cycle, is restartable and throttable between 40 and 100 % nominal thrust [12]. Further studies demonstrated an increased throttle range between 21 and 109 % [13]. By-passing the turbopumps allows operation in "idle mode" [14]. A summary on the RSR engine which will be used in a modified version for CALLISTO can be found in [15]. For all presented calculations 110% thrust level was assumed (see table 1).

Table 1. Engine conditions [12, 15, 16]. ND: not disclosed.

Condition	110 %	nominal (100 %)
Thrust	44 kN	40 kN
Specific impulse (sea level)	ND	320 s
Mixture ratio	ND	6
Chamber pressure	ND	34 bar
Chamber temperature	approx. 3500 K	ND

The influence of plume chemistry and turbulence model was investigated during an early phase B study. For an approximate 2D configuration based on CAL1B geometry[8] the influence of the Spalart-Allmaras, k-ω SST and RSM turbulence models were investigated preliminary along with plume chemistry based on finite rate chemistry models[9]. While the chemistry plays a minor role, the influence of the turbulence closure is more crucial and motivates this study.

2.2. CALLISTO thermal interfaces

For use in the CALLISTO design process and loads definition, thermal interfaces (tanks, legs, etc..) for the entire vehicle were defined. The number of interfaces varies by configuration, with more interfaces being

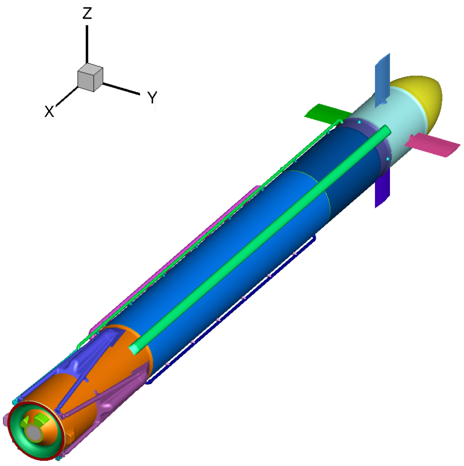

Figure 3. CALLISTO CAL1C vehicle: overview of thermal and aerodynamic interfaces.

present for the legs open (e.g. UUO) configuration. However for the UFO configuration used in this study we have over 50 thermal interfaces. A graphic of the thermal interfaces is shown in figure 3. The fairing and legs assemblies have multiple thermal interfaces not pictured here which are described more in detail in references [17] and [18].

3. Methodology

3.1. CFD code and turbulence modelling

All numerical investigations in the presented study were performed using the hybrid structured/unstructured DLR in-house Navier-Stokes solver TAU[19, 20]. This code is validated[21, 22] for a wide range of steady and unsteady sub-, trans[23]- and hypersonic[24] flow cases. It is a second order finite-volume solver for the Euler and Navier-Stokes equations in the integral form using eddy-viscosity, Reynolds-stress or detached- and large eddy simulation for turbulence modelling. TAU allows for the computation of flows in thermal and chemical equilibrium and non-equilibrium.

The main focus of the presented study was using the hybrid RANS LES approach IDDES [25] in order to get a better understanding of the physical limitations of the standard RANS models for this application as there is no wind tunnel data available for UFO configuration. The IDDES method is an improved version of the Detached Eddy Simulation (DES) method originally proposed by Spalart[26]. As such it is a zonal combination of Large Eddy Simulation (LES) with unsteady Reynolds-Averaged Navier-Stokes (URANS). The zones or regions in which either model is applied depends on a length scale criterion. The zones with the turbulent length scale smaller than the cut-off scale use RANS modelling, while the zones with the turbulent length scale larger than the cut-off use LES modelling. The LES regions are situated where flow is dominated by large-scale, unsteady turbulent structures. The Delayed Detached Eddy Simulation (DDES) model tries to improve on DES by adding a a delay function which slows down the transition from RANS to LES. Further improvements were made with the IDDES model by adding an advanced blending function to address the log-layer mismatch problem in DDES[27].

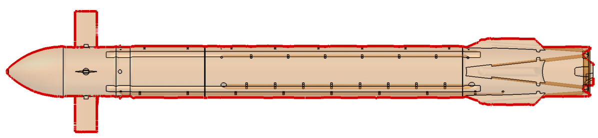

Figure 4. Distribution of zones. RANS mode is active very close to the wall, the boundaries are indicated with a red line.

IDDES has found more and more application in recent numerical studies of scramjets[28] but also first stage launchers [29]. Additionally to the IDDES modelling, both the Callisto baseline turbulence model Spalart-Allmaras (SA original)[30] as well as Menter k-ω SST[31] turbulence models were used. As convergence for the Menter k-ω SST was very challenging, this model was mainly used in the unsteady mode (URANS). The RANS formulation of the IDDES simulation also uses the SA model. An improved Advection Upstream Splitting Method (AUSMDV [32]) flux vector splitting scheme was applied together with Monotonic Upstream-centered Scheme for Conservation Laws (MUSCL [33]]) gradient reconstruction to achieve second order spatial accuracy.

3.2. Thermo-chemistry model and boundary conditions

The thermo-chemistry model for this study is based on a two species frozen gas model (frozen at nozzle exit) as described in in detail in Ecker et al.[9]. The nozzle exit conditions are applied as a Dirichlet boundary condition using the nozzle exit results from a 2D-nozzle chemical non-equilibrium calculation of the CALLISTO vehicle at 110% thrust condition. This condition can be found in table 1. All heat flues are given in Terms of Nusselt number (Nu) based on aeroshell wall temperature and engine chamber temperature for reference temperature (compare table 1).

The Nusselt number is defined as:

$$Nu = \frac{qL}{k * (T_{cc} - T_{\infty})} \tag{1}$$

where q is the heat flux (units: W/m^2) , L the characteristic length (d = 1.1 m), k the thermal conductivity (units: kg m s^{-3} K^{-1}) of air and T_{cc} the combustion chamber temperature (units: K) and T_{∞} the wall temperature (units: K).

3.2.1. Mesh

The UFO mesh configuration is visualized in figure 5. Grid refinement is applied to the near vehicle volumes and in the area of the plume. The mesh contains over 23 Mio points (about 65 Mio elements) as well as almost 100k surface elements. The same mesh is used for IDDES as well as RANS and URANS studies. Calculation time for the IDDES simulation was about 3 months on 3200 CPUs for 0.4 s of flow time.

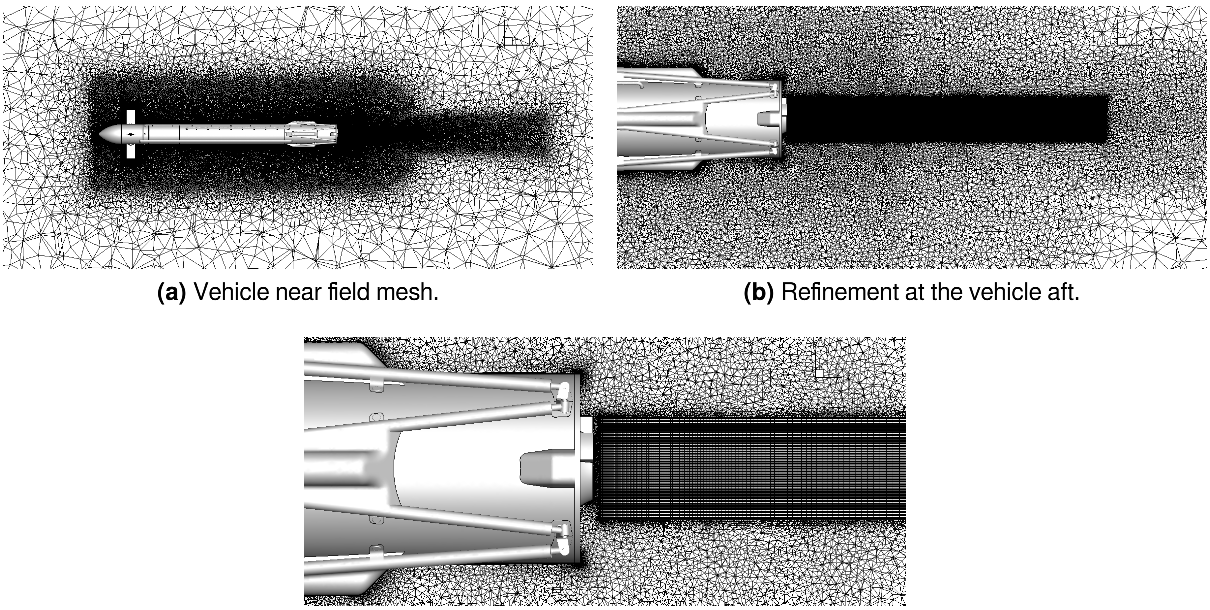

(a) Vehicle near field mesh.

(b) Refinement at the vehicle aft.

(c) Detail of structured block at the nozzle exit.

Figure 5. Visualisation of mesh details .

4. Results

4.1. Flight condition

For the flight condition investigated we choose a condition close to the maximum Mach number within the aerothermal database parameter space. While higher Mach numbers are contained within this database limitations arise from the engine restart procedure. The conditions are listed in table 2. For the IDDES data was collected for 0.4 s of flow time, however a start up period of 0.1 s (approx. 20 vehicle lengths of flow) was excluded from the statistics. The timestep was set at 1 μs.

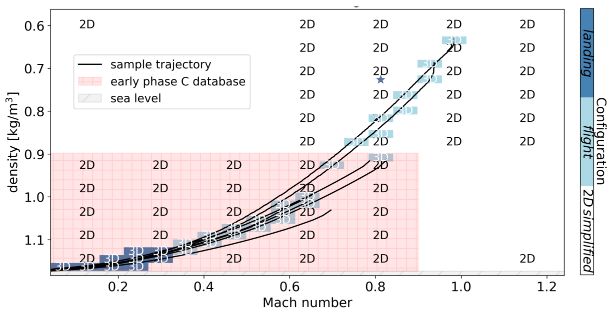

Figure 6. Aerothermal database domain with sample trajectories (from [9]). DES flight condition marked with blue star.

Table 2. Flight condition

Variable	value
Mach number	0.8
Density	0.72065 kg/m^3
Temperature	254.36 K
Angle of attack	175 deg

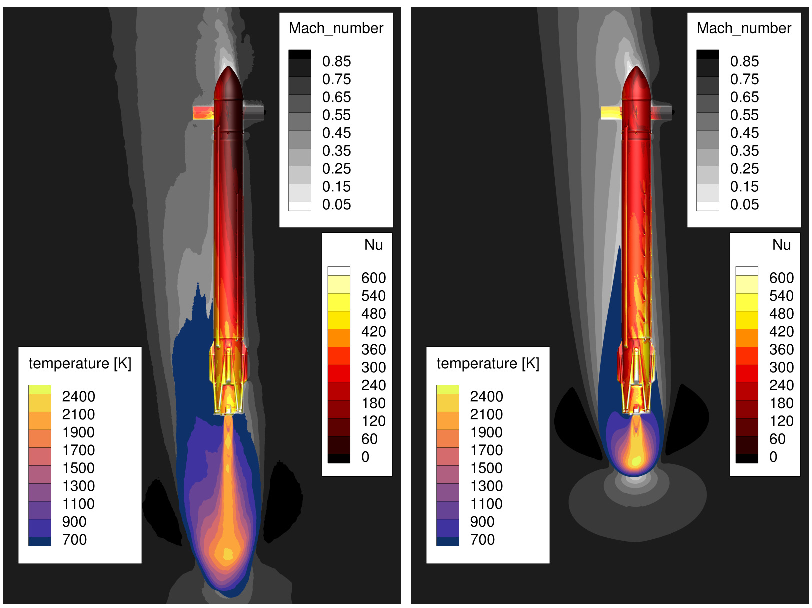

(a) DES mean temperature

(b) SA temperature

Figure 7. Gas temperature (plume), Nu Number on surface and Mach contours (grey scale)

An average of Mach and temperature distribution of the IDDES and the RANS calculation in shown in figure 7. While the general flow field is similar, some differences arise. Firstly the plume of the IDDES is significantly longer, secondly the thermal loads show significantly lower magnitudes especially along the fuselage and fairing. A detailed comparison of the system vehicle interface thermal loads is given in section 4.4.

4.2. IDDES snapshots

In order to give an impression on the plume dynamics we visualized the plume and vehicle thermal loads in spaced snapshots as shown in figure 8. From these few snapshots, spaced 20 ms (approx. a fluid particle travels about half a vehicle length at the free-stream velocity) two essential points can be demonstrated. The plume length is not static but varies throughout the subsonic retro-burn with the stagnation point moving up to two vehicle diameters. Further the thermal loads on the vehicle fuselage encounter a large variation over time, sections of very hot exhaust gases alternate with cold freestream air, leading to rapidly changing thermal environments for parts of the vehicle.

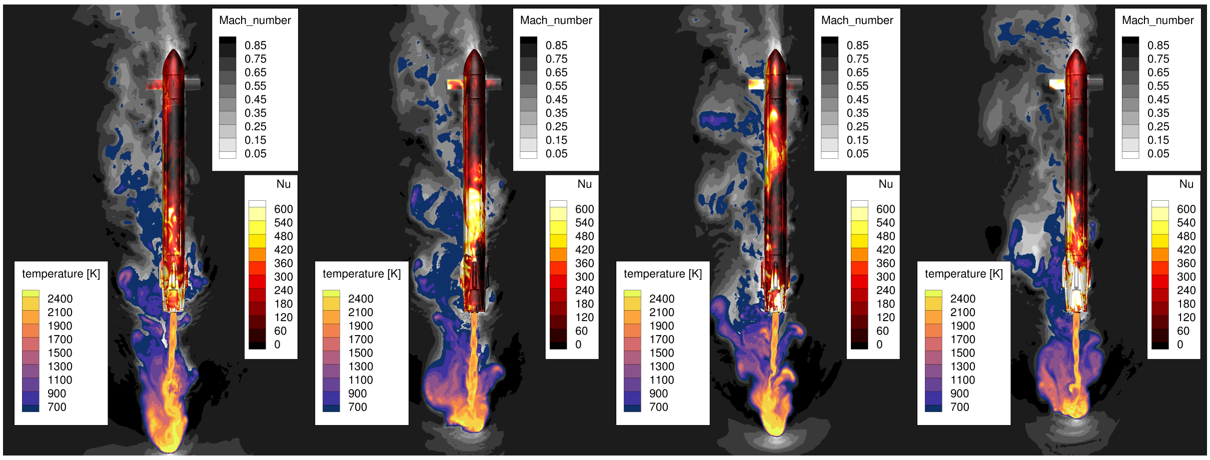

(a) 0.26 s **(b)** 0.28 s **(c)** 0.30 s **(d)** 0.32 s

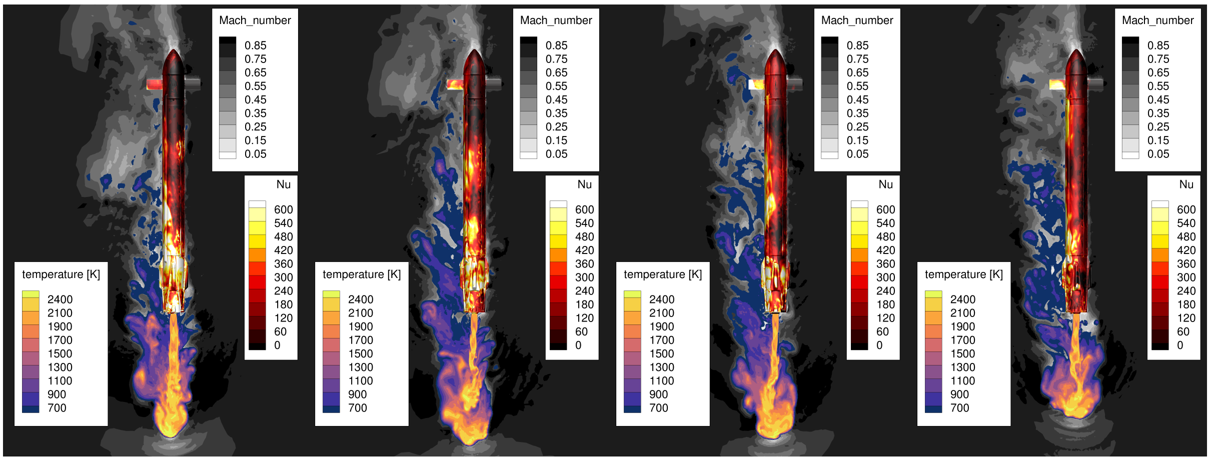

(e) 0.34 s **(f)** 0.36 s **(g)** 0.38 s **(h)** 0.40 s

Figure 8. Temperature and heat flux snap shots from IDDES.

4.3. Global and pressure coefficients

Properly modelling free jets is a known issue for almost all RANS models, albeit it seems to be a smaller issue for supersonic retro-propulsion. Just like the flow field shown earlier, the global coefficients from IDDES, especially for the drag and x coefficient show large discrepancy when compared to the RANS results from the SA model. An time resolved magnitude of the global aerodynamic coefficients and the respective mean and baseline values are given in figure 9. This difference in drag is not unexpected as the base drag heavily contributes to the total drag. While the RANS model predicts negative drag, the IDDES shows positive drag which would be beneficial to the deceleration of the vehicle during the retro-burn.

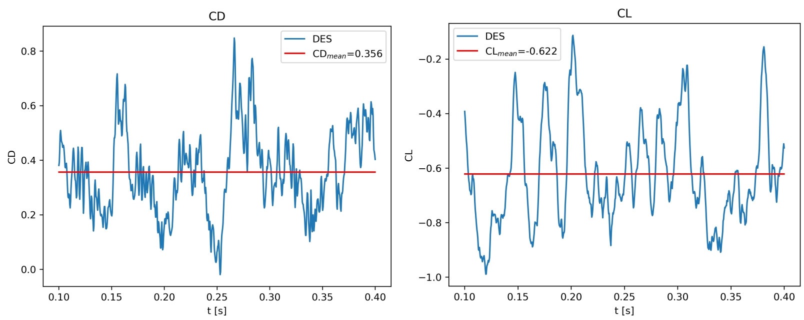

(a) C$_D$ (SA) = -0.1618 **(b)** C$_L$ (SA) = -0.4814

Figure 9. Drag and lift coefficients.

Beneficial to understanding where the unsteady dynamics of the plume or the flow in general play a role is to look at the RMS pressure cost-efficient defined as:

$$C_p = \frac{P - P_\infty}{0.5\rho_\infty U_\infty^2} \tag{2}$$

The root mean square ($RMS = \sqrt{(\frac{1}{n})\sum_{i=1}^{n}(Cp_i)^2}$) of the distributed C_p values are indicative of the effective pressure the vehicle encounters during subsonic retro-propulsion.

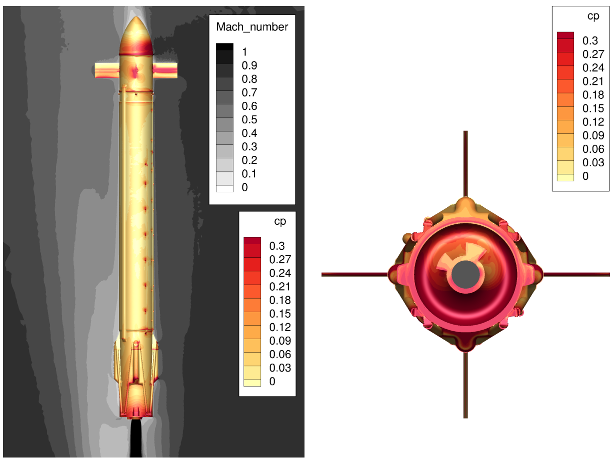

(a) side **(b)** base

Figure 10. RMS surface pressure loads.

The surface C_p RMS distribution for the fuselage and the base is shown in figure 10. The highest values are present on the base and on the fairing and are about 0.3 which is similar to what was reported experimentally[7] for a launcher configuration for the shoulder and base area.

4.4. Thermal loads comparison with baseline and IDDES

In order to allow a system level comparison of thermal loads between the RANS baseline and the IDDES, the time resolved area averaged data (for each interface) is compared in the mean and for RMS values. The comparison is shown in figure 11. The time-averaged results show a qualitative similar distribution to the RANS results for this flight conditions.

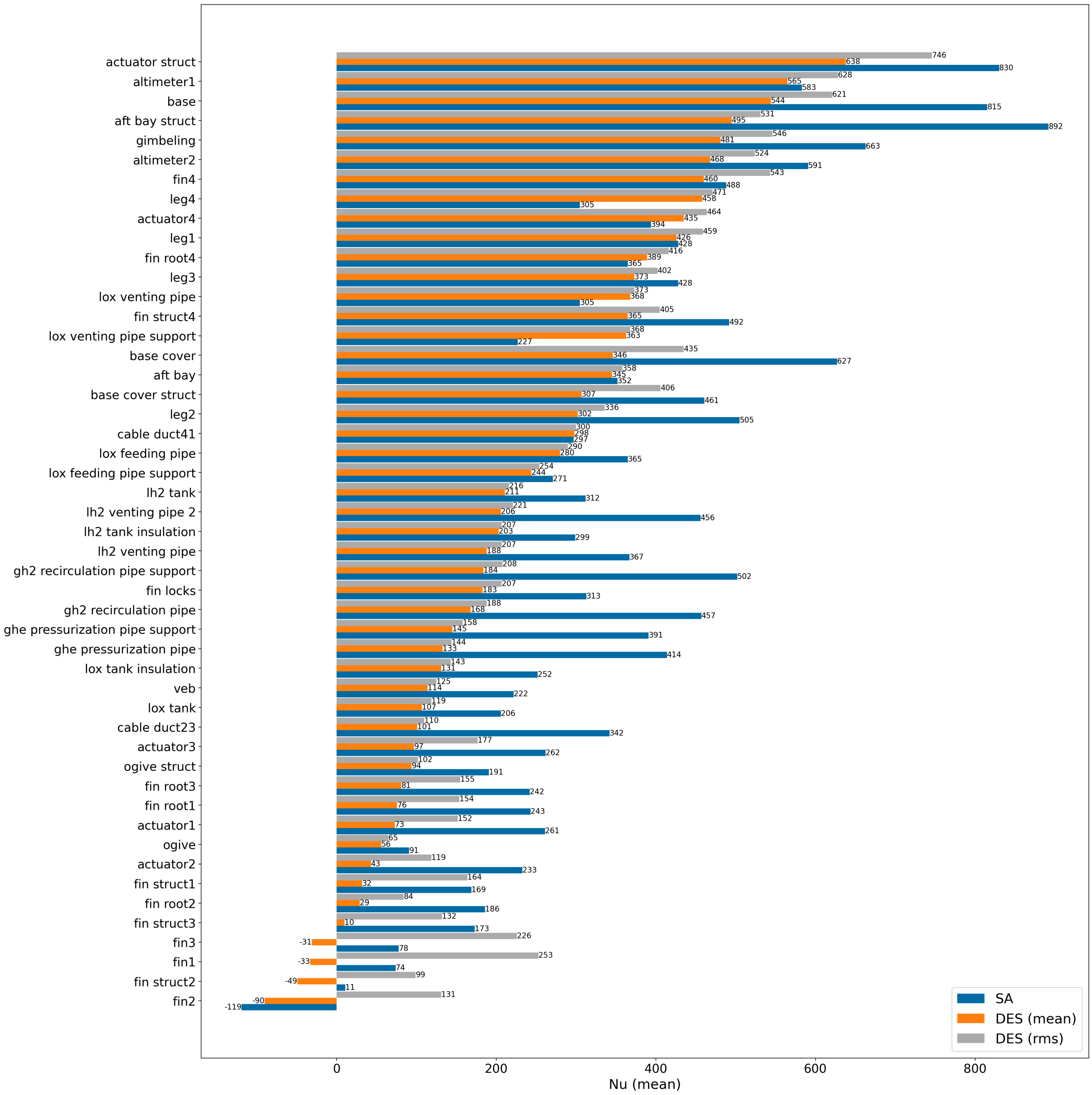

Figure 11. Comparison of DES mean values with baseline thermal loads.

In general thermal loads predicted from the IDDES are lower across all interfaces and almost never exceed (asides the LOX venting pipe support which is a very small interface) the baseline prediction based on the SA model. In conclusion the thermal loads from the SA model can be seen as conservative (in the mean) but might also contributing to increased TPS mass and lower performance. Based on the observation of the time-resolved thermal loads (compare figure 8) the particular interfaces might see much higher instantaneous heat fluxes compared to mean or RMS value. The impact of these loads depends strongly of the material properties and the mass of the vehicle structure as well as the chosen thermal protection system.

5. Conclusions

As the UFO configuration (plume on) could not be easily tested in the past windtunnel campaigns both aerothermal and aerodynamics predictions suffer from higher uncertainties. In the current study we present the first results of a improved Detached Eddy Simulation of the Callisto vehicle during subsonic retro-propulsion. In this study we focus on the loads on the vehicle at beginning of the demo flight powered descent at M=0.8. The study was conducted for 0.3 s of flow time after the start up period. As typical RANS turbulence models struggle with properly modelling free jets and their associated quantities like plume length scale resolving methods like LES and DES are expected to better predict these type of flows. From the IDDES the time-averaged loads were evaluated and compared to the baseline RANS model for the flowfield and the different systems engineering vehicle interfaces. The IDDES shows a significantly longer plume and strong differences in the vehicle drag which may positively impact vehicle performance. While large scale turbulent structures heavily influence the instantaneous thermal loads on the different vehicle interfaces the time-averaged thermal loads show a qualitative similar distribution to the RANS results for the same conditions. However the impact of the higher instantaneous loads may strongly depend on the material properties and the thermal mass of the underlying structure and the TPS system.

Acknowledgements

The author gratefully acknowledges the scientific support and HPC resources provided by the German Aerospace Center (DLR). The HPC system CARO is partially funded by “Ministry of Science and Culture of Lower Saxony“ and „Federal Ministry for Economic Affairs and Climate Action”. The CALLISTO project is funded by the „Federal Ministry for Economic Affairs and Climate Action” on the basis of a decision of the German parliament. Further I would like to acknowledge Dr. Josef Klevanski and Sven Krummen for the support in conducting this research.

Gefördert durch:

Bundesministerium
für Wirtschaft
und Klimaschutz

aufgrund eines Beschlusses
des Deutschen Bundestages

References

1. Bykerk, T., Karl, S., Ertl, M., Laureti, M. & Ecker, T. Retro-propulsion in rocket systems: Recent advancements and challenges for the prediction of aerodynamic characteristics and thermal loads - ScienceDirect. *Progress in Aerospace Sciences* **151** (ed ScienceDirect) 1–32 (Nov. 2024).
2. Dumont, E., Ishimoto, S., Illig, M., Sagliano, M., Solari, M., Ecker, T., Martens, H., Krummen, S., Desmariaux, J., Saito, Y., Ertl, M., Klevanski, J., Reimann, B., Woicke, S., Schwarz, R., Seelbinder, D., Markgraf, M., Riehmer, J., Braun, B. & Aicher, M. *CALLISTO: towards reusability of a rocket stage: current status* in *33rd ISTS Conference* (Mar. 2022).
3. Korzun, A. M., Cordell Jr, C. E. & Braun, R. D. Computational aerodynamic predictions of supersonic retropropulsion flowfields. *Journal of Spacecraft and Rockets* **50,** 950–960 (2013).

4. Marwege, A. & Gülhan, A. Unsteady Aerodynamics of the Retropropulsion Reentry Burn of Vertically Landing Launchers. *Journal of Spacecraft and Rockets* (Aug. 2023).
5. Bykerk, T. & Karl, S. *Preparatory CFD Studies for Subsonic Analyses of a Reusable First Stage Launcher during Landing within the RETPRO Project* in *10th EUCASS – 9th CEAS Conference 2023* (eds EUCASS & CEAS) (July 2023), 1–10.
6. Marwege, A., Kirchheck, D. & Gülhan, A. *First Hot Combustion Subsonic Retro Propulsion Tests in the Vertical Free Jet Facility Cologne (VMK)* in *HiSST: 3rd International Conference on High-Speed Vehicle Science Technology* (Apr. 2024).
7. Marwege, A. & Gülhan, A. Aerodynamic Characteristics of the Retro Propulsion Landing Burn of Vertically Landing Launchers. *Experiments in Fluids* **65** (Aug. 2024).
8. Klevanski, J., Ecker, T., Riehmer, J., Reimann, B., Dumont, E. & Chavagnac, C. *Aerodynamic Studies in Preparation for CALLISTO - Reusable VTVL Launcher First Stage Demonstrator* in *69th International Astronautical Congress (IAC)* IAC-18- D2.6.3 (Oct. 2018).
9. Ecker, T., Ertl, M., Klevanski, J., Krummen, S. & Dumont, E. Aerothermal characterization of the CALLISTO vehicle during descent. *CEAS Space Journal. High-Speed Vehicle Science and Technology* (ed Link, S.) 1–20 (Aug. 2024).
10. Klevanski, J., Reimann, B., Krummen, S., Ertl, M., Ecker, T., Riehmer, J. & Dumont, E. *Progress in Aerodynamic Studies for CALLISTO - Reusable VTVL Launcher First Stage Demonstrator* in *9th European Conference for Aeronautics and Space Sciences (EUCASS)* (June 2022).
11. Ertl, M. & Ecker, T. *Aerodynamic and aerothermal comparison between the CAL1C and CAL1D geometries for the CALLISTO vehicle* in *10th EUCASS - 9th CEAS 2023* (eds EUCASS & CEAS) (July 2023), 1–12.
12. SATO, M., HASHIMOTO, T., TAKADA, S., KIMURA, T., ONODERA, T., NARUO, Y., YAGISHITA, T., NIU, K.-i., KANEKO, T. & OBASE, K. Development of Main Propulsion System for Reusable Sounding Rocket: Design Considerations and Technology Demonstration. *TRANSACTIONS OF THE JAPAN SOCIETY FOR AERONAUTICAL AND SPACE SCIENCES, AEROSPACE TECHNOLOGY JAPAN* **12** (2014).
13. Kimura, T., Hashimoto, T., Sato, M., Takada, S., Moriya, S.-i., Yagishita, T., Naruo, Y., Ogawa, H., Ito, T., Obase, K. & Ohmura, H. Reusable Rocket Engine: Firing Tests and Lifetime Analysis of Combustion Chamber. *Journal of Propulsion and Power* **32,** 1087–1094 (2016).
14. Desmariaux, J., CLIQUET-MORENO, E., Chavagnac, C., Dumont, E. & Saito, Y. *CALLISTO: Its Flight Envelope and Vehicle Design* in *8th European Conference for Aeronautics and Space Sciences (EUCASS), Madrid, Spain* (July 2019).
15. Ishimoto, S., Tatiossian, P. & Dumont, E. *Overview of the CALLISTO Project* in *32nd ISTS and NSAT* (June 2019).
16. Kimura, T., Hashimoto, T., Sato, M., Takada, S., Moriya, S.-i., Yagishita, T., Naruo, Y., Ogawa, H., Ito, T., Obase, K. & Ohmura, H. Reusable Rocket Engine: Firing Tests and Lifetime Analysis of Combustion Chamber. *Journal of Propulsion and Power* **32,** 1–8 (Apr. 2016).
17. Vincenzino, S. G., Eichel, S., Rotärmel, W., Krziwanie, F., Petkov, I., Dumont, E., Schneider, A., Schröder, S., Windelberg, J., Ecker, T. & Ertl, M. *Development of Reusable Structures and Mechanisms for CALLISTO* in *33rd ISTS Conference* (Mar. 2022).
18. Ertl, M., Ecker, T., Klevanski, J., Krummen, S. & Dumont, E. *Aerothermal analysis of plume interaction with deployed landing legs of the CALLISTO vehicle* in *9th European Conference for Aeronautics and Space Sciences* (2022).
19. Langer, S., Schwöppe, A. & Kroll, N. The DLR Flow Solver TAU – Status and Recent Algorithmic Developments. *AIAA Paper AIAA-2014-0080. 52nd Aerospace Sciences Meeting* (2014).
20. Schwamborn, D., Gerhold, T. & Heinrich, R. *The DLR TAU-code: recent applications in research and industry* in *ECCOMAS CFD 2006: Proceedings of the European Conference on Computational Fluid Dynamics, Egmond aan Zee, The Netherlands, September 5-8, 2006* (2006).
21. Schwamborn, D., Gerhold, T. & Hannemann, V. in *New Results in Numerical and Experimental Fluid Mechanics II: Contributions to the 11th AG STAB/DGLR Symposium Berlin, Germany 1998* (eds Nitsche, W., Heinemann, H.-J. & Hilbig, R.) 426–433 (Vieweg+Teubner Verlag, Wiesbaden, 1999).

22. Cambier, L. & Kroll, N. MIRACLE – a joint DLR/ONERA effort on harmonization and development of industrial and research aerodynamic computational environment. *Aerospace Science and Technology* **12,** 555–566 (2008).
23. Knopp, T. *Validation of the turbulence models in the DLR TAU Code for transonic flows. A best practice guide* Feb. 2006.
24. Mack, A. & Hannemann, V. in *32nd AIAA Fluid Dynamics Conference and Exhibit* ().
25. Shur, M. L., Spalart, P. R., Strelets, M. K. & Travin, A. K. A hybrid RANS-LES approach with delayed-DES and wall-modelled LES capabilities. *International Journal of Heat and Fluid Flow* **29,** 1638–1649 (2008).
26. Spalart, P. R. *Comments on the Feasibility of LES for Wings and on the Hybrid RANS/LES Approach* in *Proceedings of the First AFOSR International Conference on DNS/LES, 1997* (1997), 137–147.
27. Spalart, P. R., Deck, S., Shur, M. L., Squires, K., Strelets, M. K. & Travin, A. A new version of detached-eddy simulation, resistant to ambiguous grid densities. English (US). *Theoretical and Computational Fluid Dynamics* **20,** 181–195 (July 2006).
28. Yao, W., Liu, H., Xue, L. & Xiao, Y. Performance analysis of a strut-aided hypersonic scramjet by full-scale IDDES modeling. *Aerospace Science and Technology* **117,** 106941 (2021).
29. Bykerk, T. & Horchler, T. *CFD Analysis of a Re-Usable First Stage in the Transonic Regime* in *24th Australasian Fluid Mechanics Conference – AFMC2024* (Dezember 2024), 1–8.
30. Spalart, P.R. & Allmaras, S.R. A One-Equation Turbulence Model for Aerodynamic Flows. *AIAA Paper AIAA-92-0439* (1992).
31. Menter, F. R. Two-equation eddy-viscosity turbulence models for engineering applications. *AIAA Journal* **32,** 1598–1605 (1994).
32. Wada, Y. & Liou, M.-S. An Accurate and Robust Flux Splitting Scheme for Shock and Contact Discontinuities. *SIAM Journal on Scientific Computing* **18,** 633–657 (1997).
33. van Leer, B. Towards the ultimate conservative difference scheme. V. A second-order sequel to Godunov's method. *Journal of Computational Physics* **32,** 101–136 (1979).